Contrast Agents

DOI: 10.1002/anie.201007018

Controlled Self-Assembling of Gadolinium Nanoparticles as Smart Molecular Magnetic Resonance Imaging Contrast Agents**

*Gaolin Liang, John Ronald, Yuanxin Chen, Deju Ye, Prachi Pandit, Man Lung Ma, Brian Rutt, and Jianghong Rao**

In recent years, contrast-enhanced magnetic resonance imaging (MRI) has shown promise for in vivo visualization of reporter gene expression and molecular biomarkers of various diseases.[1] MRI can provide high-resolution images of the entire body with exquisite image contrast. However, compared to other imaging modalities, MRI has relatively poor sensitivity to low levels of molecular targets, and therefore the design of highly potent molecular probes is crucial for success.[2] "Smart" or "activatable" probes that modulate their MR properties (relaxivity) resulting in signal amplification upon molecular target interaction can greatly help improve MRI detection of specific molecular events. A few gadolinium-based smart probes have been developed, including those that are responsive to β-galactosidase and myeloperoxidase.[3] Herein we present the rational design of a new, potentially generalized smart MR probe platform based on a biocompatible and controllable condensation reaction between a 1,2-aminothiol and 2-cyanobenzothiazole (CBT).

This condensation reaction has been shown to occur in vitro and in living cells under the control of a variety of physiological conditions, including pH change, disulfide reduction, or enzymatic cleavage, to synthesize nanoparticles with diameters ranging from 8 nm to 170 nm.[4] We envisioned that a CBT-based, gadominium-containing "smart" probe could similarly condense to produce more hydrophobic oligomers that self-assemble to form gadolinium-containing nanoparticles (Gd NPs) in response to the molecular target. These assembled Gd NPs should have relaxivity enhancement compared with that of the precursor with an identical Gd concentration.

As the proof-of-principle demonstration of our smart MRI probe concept, we designed the probe **1** that could be activated by disulfide reduction (Scheme 1). Thiol redox chemistry is central to the control of cell fate and is associated with various abnormal biochemical processes.[5] Probe **1** contains the MR moiety DOTA-Gd chelate for MR imaging. Disulfide reduction either by tris(2-carboxyethyl)phosphine (TCEP) in vitro or glutathione (GSH) in cells generates an intermediate with a free 1,2-aminothiol group. This 1,2-aminothiol reacts with the cyano group on the CBT motif to initiate condensation leading to the formation of larger, more hydrophobic molecules (that is, oligomers), which self-assemble to form nanoparticles with enhanced relaxivity, presumably owing to an increased rotational correlation time (Scheme 1).

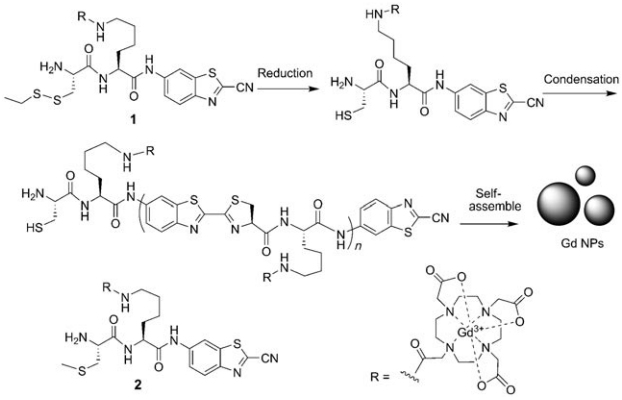

Scheme 1. Reduction-controlled condensation of **1** to assemble gadolinium-containing nanoparticles (Gd NPs). Compound **2** is the control probe that cannot be reduced to induce condensation.

A 1 mM solution of **1** is obtainable in 0.2 M phosphate buffer. When treated with 4 mM TCEP at RT for 1 h, condensation of **1** occurs to afford cyclized dimeric, trimeric, tetrameric, and higher-order oligomers, as detected by matrix-assisted laser desorption/ionization (MALDI) mass spectrometry (Figure 1). UV/Vis spectra recorded at 500–700 nm and dynamic light scattering (DLS) measurements consistently showed the aggregation of particles with a mean diameter of 275 nm (Supporting Information, Figure S4).

[*] Dr. G. Liang,[+] Dr. J. Ronald,[+] Dr. D. Ye, Dr. P. Pandit, M. L. Ma, Prof. B. Rutt, Prof. J. Rao
Molecular Imaging Program at Stanford
Department of Radiology, Stanford University
1201 Welch Road, Stanford, CA 94305-5484 (USA)
Fax: (+1) 650-736-7925
E-mail: jrao@stanford.edu
Homepage: http://raolab.stanford.edu
Dr. Y. Chen
Imaging Research Laboratories, Robarts Research Institute
The University of Western Ontario
100 Perth Drive, London N6A 5K8 (Canada)
Dr. G. Liang[+]
Department of Chemistry
University of Science and Technology of China
96 Jinzhai Road, Hefei, Anhui 230026 (China)
[+] These authors contributed equally to this work.

[**] This work has been supported by the CCNE-T, a grant funded by National Cancer Institute (NCI) (1U54CA151459), and the NCI ICMIC@Stanford (1P50CA114747-06). P.P. is supported by a Stanford Molecular Imaging Scholars (SMIS) fellowship and J.R. by a Canadian Institute of Health Research Post-Doctoral Fellowship. We thank Dr. Richard Chin for assistance with the EDX experiment.
Supporting information for this article is available on the WWW under http://dx.doi.org/10.1002/anie.201007018.

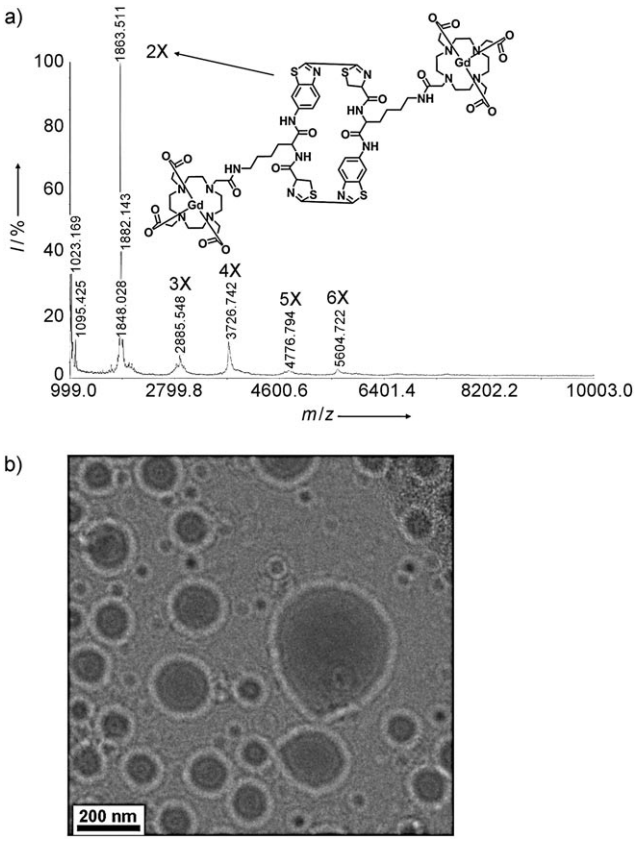

Figure 1. a) MALDI mass spectrum of the oligomer mixtures of **1** after TCEP reduction. b) Representative TEM image of the condensation products of **1** in 0.2 M phosphate buffer (pH 7.4) treated with 4 mM TCEP.

Transmission electron microscope (TEM) images revealed the shapes of separated Gd NPs with diameters ranging from 100 nm to 360 nm (Figure 1). The presence of Gd was confirmed by energy-dispersive X-ray (EDX) spectroscopy (Supporting Information, Figure S4d). Apart from the nanoparticles, the DLS data also showed particles with a mean diameter of 2.1 μm, which are most likely due to further aggregation of some nanoparticles at this concentration (1 mM), consistent with the TEM observation (Supporting Information, Figure S4c). Under the same conditions, the control probe **2** whose thiol group was methylated could not be reduced by TCEP to form condensation products detected by HPLC and UV/Vis spectroscopy (Supporting Information, Figure S5).

Nuclear magnetic relaxation dispersion (NMRD) is a technique to measure the longitudinal relaxation rate R_1 of water protons in solution as a function of NMR field strength, or, equivalently, Larmor frequency. NMRD can be used to study dynamics in condensed matter as the longitudinal relaxation time T_1 ($T_1 = 1/R_1$) is determined by fluctuations in local fields. At 768 μM in 0.2 M phosphate buffer (pH 7.4) and different temperatures ranging from 5 to 35 °C in the absence of TCEP, both **1** and **2** have decreased relaxation rates as either the temperature or the magnetic field is increased (Supporting Information, Figure S6a,c). These NMRD profiles are typical of those measured from solutions of small-molecule paramagnetic complexes; the shape is governed by a combination of rotational correlation time of the complex and the exchange rate of the inner-sphere coordinated water molecule.[6] Importantly, after adding TCEP, the profiles of the above two solutions are clearly different. The NMRD profile of **2** with TCEP remained nearly unchanged compared to **2** without TCEP, suggesting no change in rotational correlation time or coordinated water exchange rate and this observation is consistent with the absence of nanoparticle formation (Supporting Information, Figure S6d). In contrast, the solution of **1** with TCEP showed increased relaxation rates upon the increase of temperature, and a broad hump appeared in the NMRD profile from 8.4 to 127.7 MHz (0.2 to 3 T), suggesting changes in rotational correlation time owing to the formation of nanoparticles with measurable sizes in the solution (Supporting Information, Figure S6b).[7] Figure 2a shows the NMRD profiles of **1** in 0.2 M phosphate buffer (pH 7.4) before and after condensation by TCEP at 35 °C. At 25.6 MHz (ca. 0.6 T), the relaxation rate of **1** after condensation increased by 160 % compared to **1** before condensation. At 64 MHz (1.5 T), the relaxation rate increased by 110 %

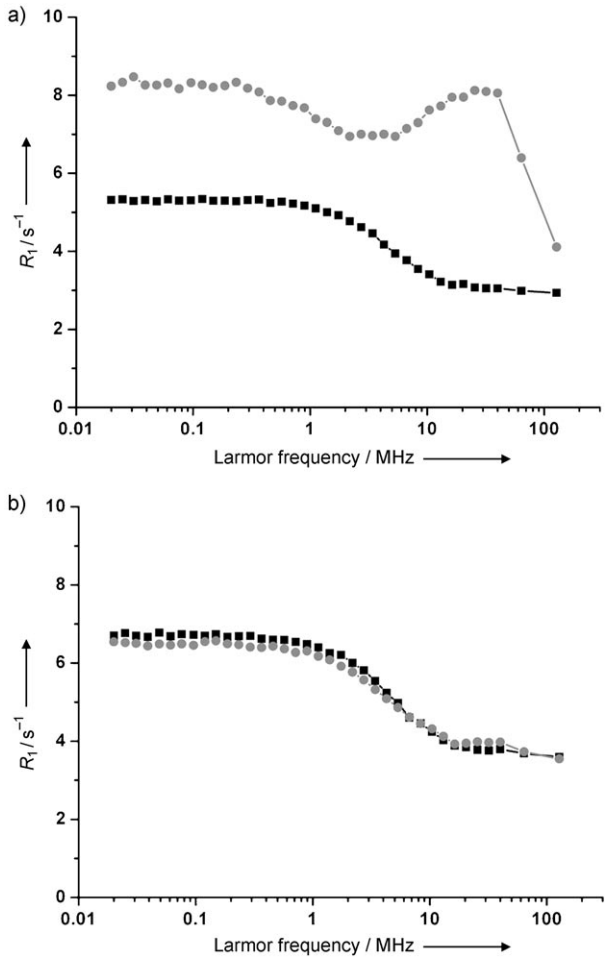

Figure 2. NMRD profiles of a) **1** and b) **2** treated with (●) and without (■) 4 mM of TCEP at 35 °C. R_1 = longitudinal relaxation rate. Concentrations of **1** and **2**: 768 μM in 0.2 M phosphate buffer (pH 7.4).

after condensation. In contrast, the relaxation rate of **2** did not obviously change before and after TCEP addition (Figure 2b).

We also conducted T_1-weighted MR imaging of **1** and **2** with and without TCEP on both 1.5 T and 3 T MRI scanners (Supporting Information, Figure S7). Plots of signal intensity versus inversion time clearly showed that after TCEP reduction **1** had a shortened T_1 relaxation time, while **2** did not (Supporting Information, Figure S7c,d). Using inductively coupled plasma atomic emission spectroscopy (ICP-AES) to measure the concentration of Gd^{3+} in the imaged samples, we calculated the relaxivity of each probe according to the equation $r_1 = \Delta R_1/[\text{concentration}]$. At 35 °C and 1.5 T, the relaxivity of **1** is 3.9 $mM^{-1}s^{-1}$ and the relaxivity of its assembled products increases to 8.3 $mM^{-1}s^{-1}$. In contrast, the relaxivities of **2** before and after TCEP addition at 35 °C and 1.5 T remained nearly the same (4.8 and 4.9 $mM^{-1}s^{-1}$, respectively). These results indicate that, after condensation, the relaxivity of **1** is dramatically enhanced owing to the formation of GdNPs. Similarly, the relaxivity of **1** at 3 T increased by 40% after the TCEP addition (5.4 versus 3.8 $mM^{-1}s^{-1}$) and the relaxivity of **2** changed little before and after TCEP addition (4.7 and 4.6 $mM^{-1}s^{-1}$, respectively).

We next measured the relaxivity of **1** and **2** in the lysate of MDA-MB-468 cells (Supporting Information, Figure S8). The relaxivities of both **1** and **2** in the cell lysate at 1.5 T are higher than that in TCEP-treated buffer (14.8 versus 8.3 $mM^{-1}s^{-1}$ for **1**, and 10.5 versus 4.9 $mM^{-1}s^{-1}$ for **2**). Consistent with the increase in the relaxivity after the TCEP reduction, the relaxivity of **1** in the cell lysate is also 40% higher than that of **2** at 1.5 T and 35 °C (14.8 versus 10.5 $mM^{-1}s^{-1}$). HPLC analysis confirmed that cell lysate could similarly induce the condensation of **1** as for TCEP and produce the cyclic oligomers (Supporting Information, Figure S9).

We tested the cell permeability of **1** by directly imaging the uptake of its europium analogue, compound **3** (Figure 3),

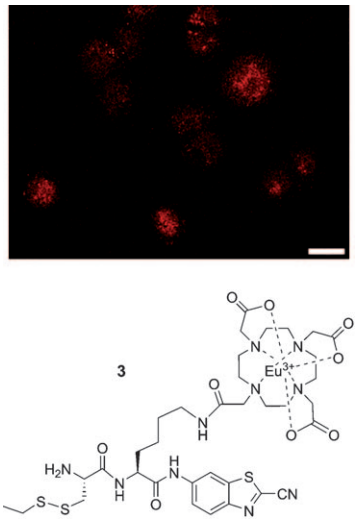

Figure 3. Structure of analogue **3** and two-photon laser microscopy image (λ_{ex} = 725 nm, λ_{em} = 565–615 nm) of MDA-MB-468 cells incubated with **3** at 192 μM for 8 h and then rinsed and fixed prior to imaging. Scale bar: 20 μm.

in live cells with two-photon laser confocal microscopy (TPLM). Europium-containing compound **3** has luminescence emissions at 594 nm and 616 nm when excited at 355 nm or with two-photon excitation at 725 nm (Supporting Information, Figure S10), as reported previously.[8] TPLM imaging of MDA-MB-468 cells incubated with **3** at 192 μM for 8 h shows a strong fluorescent signal (Figure 3). Under the same conditions, cells without **3** did not have a detectable fluorescence signal. As the replacement of Gd^{3+} in **1** should not affect cell uptake, this result suggests good cell permeability of **1**. The inductively coupled plasma atomic mass spectrometry (ICP-MS) measurement of the uptake of **1** (299 μM) after 8 h incubation in MDA-MB-468 cells showed the average gadolinium uptake of 0.074 fmol per cell and 0.137 fmol per cell after 24 h incubation, further supporting good cell permeability of **1**.

Finally, we performed T_1 relaxometry of cell pellets loaded with probes **1** and **2**. MDA-MB-468 cells were incubated with **1** (299 μM) or **2** (293 μM) for 2, 4, 8, or 24 h. Each culture dish containing approximately 4 million cells was used to form a single fixed cell pellet in a mini-NMR tube (inner diameter 2.4 mm). Inversion-recovery MRI with 10 different inversion times was performed at 0.5 T, 1.5 T, and 3 T, from which the T_1 relaxation time of each cell pellet was quantified; the number of cells per pellet was also counted. Following imaging, pellets were prepared for ICP-MS for absolute [Gd] quantification to permit calculation of T_1 relaxivity. The T_1 relaxivity is summarized in Table 1. Consistent with the results in buffer and cell lysates, the relaxivity of **1** in live cells was significantly higher than that of **2** at all of the field strengths: 104% at 0.5 T, 58% at 1.5 T, and 31% at 3 T. Both of the relaxivities of **1** and **2** at 1.5 T are similar to that in cell lysates (17.40 versus 14.8 $mM^{-1}s^{-1}$ for **1**, and 11.0 versus 10.5 $mM^{-1}s^{-1}$ for **2**), and are much higher than that in TCEP-reduced buffer (17.40 versus 8.3 $mM^{-1}s^{-1}$ for **1**, and 11.0 versus 4.9 $mM^{-1}s^{-1}$ for **2**). These results demonstrate that as we reported before,[4] the condensation reaction and probe **1** can work in live cells upon the glutathione reduction.

Table 1: The T_1 relaxivity of **1** and **2** in live cells at different field strengths.

MR field strength [T]	Relaxivity of **1** [$mM^{-1}s^{-1}$]	Relaxivity of **2** [$mM^{-1}s^{-1}$]	Change [%]
0.5	18.88	9.25	104
1.5	17.40	11.0	58
3	11.69	8.91	31

In summary, we have successfully demonstrated that the condensation reaction between 1,2-aminothiol and 2-cyanobenzothiazole can be employed to assemble GdNPs that have enhanced T_1 relaxivity compared with its small-molecular precursor in vitro and in living cells. The MR agent reported here has shown good cell permeability. As we have shown previously, further chemical modifications may allow the generation of MR probes that are responsive to a variety of molecular targets such as proteases.[4] In view of current methods of designing nanoparticles for MRI,[9] this new

approach may provide us with a new platform of developing smart molecular MR probes.

Received: November 9, 2010
Revised: April 11, 2011
Published online: May 25, 2011

Keywords: condensation reactions · controlled self-assembly · gadolinium · magnetic nanoparticles · magnetic resonance imaging

[1] a) P. Caravan, J. J. Ellison, T. J. McMurry, R. B. Lauffer, *Chem. Rev.* **1999**, *99*, 2293; b) J. M. Perez, L. Josephson, T. O'Loughlin, D. Hogemann, R. Weissleder, *Nat. Biotechnol.* **2002**, *20*, 816; c) J. Xie, K. Chen, H. Y. Lee, C. J. Xu, A. R. Hsu, S. Peng, X. Y. Chen, S. H. Sun, *J. Am. Chem. Soc.* **2008**, *130*, 7542; d) J. H. Lee, Y. M. Huh, Y. Jun, J. Seo, J. Jang, H. T. Song, S. Kim, E. J. Cho, H. G. Yoon, J. S. Suh, J. Cheon, *Nat. Med.* **2007**, *13*, 95.

[2] E. Terreno, D. D. Castelli, A. Viale, S. Aime, *Chem. Rev.* **2010**, *110*, 3019.

[3] a) A. Bogdanov, Jr., L. Matuszewski, C. Bremer, A. Petrovsky, R. Weissleder, *Mol. Imaging* **2002**, *1*, 16; b) M. Querol, A. Bogdanov, *Magn. Reson. Imaging* **2006**, *24*, 971; c) M. Querol, J. W. Chen, R. Weissleder, A. A. Bogdanov, *Org. Lett.* **2005**, *7*, 1719; d) J. W. Chen, W. Phm, R. Weisleder, A. A. Bogdanov, *Magn. Reson. Med.* **2004**, *52*, 1021; e) A. L. Nivorozhkin, A. F. Kolodziej, P. Caravan, M. T. Greenfield, R. B. Lauffer, T. J. McMurry, *Angew. Chem.* **2001**, *113*, 2987; *Angew. Chem. Int. Ed.* **2001**, *40*, 2903; f) A. Y. Louie, M. M. Huber, E. T. Ahrens, U. Rothbacher, R. Moats, R. E. Jacobs, S. E. Fraser, T. J. Meade, *Nat. Biotechnol.* **2000**, *18*, 321; g) J. A. Ronald, J. W. Chen, Y. X. Chen, A. M. Hamilton, E. Rodriguez, F. Reynolds, R. A. Hegele, K. A. Rogers, M. Querol, A. Bogdanov, R. Weissleder, B. K. Rutt, *Circulation* **2009**, *120*, 592.

[4] a) G. Liang, H. Ren, J. Rao, *Nat. Chem.* **2010**, *2*, 54; b) H. Ren, F. Xiao, K. Zhan, Y. P. Kim, H. Xie, Z. Xia, J. Rao, *Angew. Chem.* **2009**, *121*, 9838; *Angew. Chem. Int. Ed.* **2009**, *48*, 9658; c) D. Ye, G. Liang, M. L. Ma, J. Rao, *Angew. Chem.* **2011**, *123*, 2323; *Angew. Chem. Int. Ed.* **2011**, *50*, 2275.

[5] a) L. Z. Li, R. Zhou, H. N. Xu, L. Moon, T. X. Zhong, E. J. Kim, H. Qiao, R. Reddy, D. Leeper, B. Chance, J. D. Glickson, *Proc. Natl. Acad. Sci. USA* **2009**, *106*, 6608; b) F. Q. Schafer, G. R. Buettner, *Free Radical Biol. Med.* **2001**, *30*, 1191; c) R. Franco, J. Cidlowski, *Cell Death Differ.* **2009**, *16*, 1303.

[6] J. L. Major, G. Parigi, C. Luchinat, T. J. Meade, *Proc. Natl. Acad. Sci. USA* **2007**, *104*, 13881.

[7] S. H. Koenig, K. E. Kellar, *Magn. Reson. Med.* **1995**, *34*, 227.

[8] Y. Shen, M. D. Chambers, D. R. Clarke, *Surf. Coat. Technol.* **2008**, *203*, 456.

[9] a) J. Gao, G. Liang, J. S. Cheung, Y. Pan, Y. Kuang, F. Zhao, B. Zhang, X. Zhang, E. X. Wu, B. Xu, *J. Am. Chem. Soc.* **2008**, *130*, 11828; b) L. M. Manus, D. J. Mastarone, E. A. Waters, X. Q. Zhang, E. A. Schultz-Sikma, K. W. MacRenaris, D. Ho, T. J. Meade, *Nano Lett.* **2010**, *10*, 484; c) S. K. Mouli, L. C. Zhao, R. A. Omary, C. S. Thaxton, *Nat. Rev. Urol.* **2010**, *7*, 84; d) M. Zhao, L. Josephson, Y. Tang, R. Weissleder, *Angew. Chem.* **2003**, *115*, 1413; *Angew. Chem. Int. Ed.* **2003**, *42*, 1375.

